*Clays and Clay Minerals*, Vol. 63, No. 2, 110–118, 2015.

# SURFACE AND INTERFACE PROPERTIES OF LAUROYL SARCOSINATE-ADSORBED $CP^+$-MONTMORILLONITE

Saadet Yapar[1], Günseli Özdemir[1], Alejandra M. Fernández Solarte[2], and Rosa M. Torres Sánchez[2]

[1] Ege University, Engineering Faculty, Chemical Engineering Department, 35100 Bornova-İzmir, Turkey
[2] CETMIC-CCT La Plata, CIC, Camino Centenario y 506, (1897) M. B. Gonnet, Argentina

**Abstract**—Catanionic surfactant systems are used as drug-delivery vehicles and as nanocompartments in the formation of biomaterials and nanosized particles. Clay minerals are compatible with organic tissues and also have biomedical applications. The aim of the present study was to combine the properties of catanionic surfactants and clay minerals to obtain new materials with potential uses in medicine, wastewater treatment, and antibacterial applications. The surfactants chosen to make the catanionic surfactant were cetylpyridinium (CP) and lauroyl sarcosinate (SR), which interact strongly in aqueous media and cause specific aggregations such as ion-pair amphiphiles and needle- and leaf-like structures. Aside from the aqueous solution, new ternary systems are formed with different structures and properties through the addition of montmorillonite (Mnt). The surface and interlayer structures of the different Mnt-CP-SR samples prepared by using CP and SR in amounts equal to various ratios of cationic exchange capacity of the clay mineral were studied. They were also compared with the structured surfactant aggregates formed in aqueous media. The Mnt-CP-SR samples were subjected to X-ray diffraction (XRD), thermogravimetric analyses, and zeta-potential measurements to elucidate the interlayer- and external-surface structures. The XRD analyses showed the formation of a compact structure in the interlayer region resulting from the interaction between randomly oriented pyridinium and negatively charged SR head groups. The triple interactions among the Mnt surface, CP, and SR were more complex than the double interactions between the Mnt and cationic surfactant, and the CP played a dominant role in the formation of external and interlayer surface structures regardless of the amount and order of the addition of SR. The new findings support new applications for organoclays in the fields of biomedicine, remediation of polluted water, and nanocomposite materials.

**Key Words**—Catanionic Surfactant, Cetylpyridinium Chloride, Organoclay, Sodium Lauroyl Sarcosinate.

## INTRODUCTION

The ternary systems comprising cationic and anionic surfactants and water have attracted the attention of many researchers because the structures formed in the aqueous phase have potential for multifaceted application in various fields including detergency, CdS nanowire production, and biomedical applications (Kaler *et al*., 1989; Herrington *et al.*, 1993; Rädler *et al*., 1997; Lasic, 1998; Caillet *et al.*, 2000; Caruso, 2000; McKelvey *et al.*, 2000; Hentze *et al.*, 2003; Bramer *et al*., 2007). The aggregates formed in an aqueous solution by simultaneously dissolved single-tailed anionic and cationic surfactants are described as catanionic systems. These aggregates can be micelles of various forms, lamellar structures, ion-pair amphiphiles (IPA), and vesicles. The IPA are distinguished from a simple surfactant mixture where surfactant pairs with opposite charges are formed and the accompanying counterions are removed leaving two amphiphilic ions in the IPA. The distinction between the two categories will become clearer to the reader when no electrolyte is subsequently added to the dispersions because all the ionic species added will be involved in the ion-exchange equilibrium (Tondre and Caillet, 2001) and the removal of the counterions is generally achieved by ion-exchange resins. The removal of the low-molecular-weight counterions will probably cause an increase in the Debye screening length and thus the ion-pair interaction between the polar heads of oppositely charged surfactants will be stronger, which may change the total area occupied by these polar heads (Tondre and Caillet, 2001).

The similarities between the vesicles and primitive biological cells make them useful as biological-membrane models, drug-delivery vehicles, or nano-compartments for the formation of biomaterials (Caillet *et al.*, 2000; Tondre and Caillet, 2001; Fischer *et al.*, 2002). Previous work reporting spontaneous vesicle formation in aqueous mixtures of positively charged cetyltrimethylammonium tosylate (CTAT) and negatively charged sodium dodecylbenzene sulfonate (SDBS) was published by Kaler *et al*. (1989) and since then the number of articles published about catanionic mixtures has increased every year (Svenson, 2004; Zhu *et al*., 2006; Karande *et al*., 2007; Maiti *et al*., 2010; Ghosh and Dey, 2011). The solution and interfacial behavior of systems derived from sodium dodecylsulfate and n-alkyltrimethylammonium bromide homologues were

* E-mail address of corresponding author:
saadet.yapar@gmail.com
DOI: 10.1346/CCMN.2015.0630203

studied by Maiti *et al*. (2010) who reported that the equimolar mixture of IPA in water yielded precipitates in the form of coacervates which consisted of needles and complex flower-like aggregates. The interaction of sodium N-lauroyl sarcosinate with n-alkylpyridinium chloride surfactants was reported by Ghosh and Dey (2011) as the spontaneous formation of pH-dependent, stable vesicles in aqueous mixtures. Those authors observed the existence of a strong interaction between sodium N-lauroyl sarcosinate and n-cetylpyridinium chloride or n-dodecylpyridinium chloride, and the formation of thermodynamically stable unilamellar vesicles in a wide range of composition and concentration in a buffered aqueous media. The vesicular structures were stable at pH values as low as 2.0 and at a 'biological' temperature (37ºC), which indicated potential application in a wide pH range to trigger the drug release. Other vesicles formed by mixtures of sodium lauroyl sarcosinate and sorbitan monolaurate synergistically enhance skin permeability to drugs (Karande *et al*., 2007).

Clays and clay minerals have been evaluated for diverse potential applications, as pollutant adsorbents (Torres Sánchez *et al.*, 2011) for sustaining the environment, and for their use in human and veterinary medicine (Parolo *et al.*, 2010). They have large adsorption capacities, excellent mechanical and chemical properties, and are inexpensive. The replacement of interlayer metal cations of montmorillonite (Mnt) with quaternary alkylammonium salts (QAS) not only increases the hydrophobicity (Erkan *et al.*, 2010), but also expands the interlayer space (Schumann *et al.*, 2014) of the organo-montmorillonite obtained allowing it to be used in a wide range of technological applications (Ruiz-Hitzky *et al.*, 2010).

The aim of the present work was to study the structure of the ternary system consisting of anionic, sodium lauroyl sarcosinate (SR), cationic, cetylpyridinium (CP) chloride surfactants, and Na-montmorillonite. To the authors' knowledge, although the complexes formed through the simultaneous and/or stepwise adsorption of cationic and anionic surfactants onto montmorillonite (Mnt) have potential in biomedical applications, adsorption, and nanostructured material production, few investigations have been carried out (Chen *et al.*, 2008) on the organoclays formed and their structural properties. The interlayer structure and thermal stability of organoclays prepared using hexadecyltrimethylammonium bromide (HDTMAB) and sodium dodecyl sulfate (SDS) were reported by Chen *et al.* (2008). In the present study, organoclay was prepared using different cations and anions, and by different processes. By way of considering the strong interaction between these surfactants, the internal and external structures and thermal behavior of the organoclay were studied. The synthesis route involved the immobilization of SR and CP on Mnt using two different processes. In the first, CP was adsorbed on the Mnt surface and SR was added later. In the second, SR and CP were mixed in an aqueous medium and were immobilized on the Mnt. The montmorillonite surface is expected to play a role similar to ion-exchange resins. In both cases, the $Cl^-$ anion will be removed from $CP^+$ through adsorption on the negatively charged surface and neutralizing ions at the interface, and the $Na^+$ cation from SR through the interaction with the $Cl^-$ anion in the medium. The samples were characterized using X-ray diffraction (XRD), thermogravimetric (TG) analyses, and zeta-potential measurements. The aggregation of CP-SR in the aqueous solution having the same proportions as used for the Mnt-CP-SR sample preparation was also studied by means of polarized optical microscope (POM) images.

## EXPERIMENTAL

### *Materials used*

The montmorillonite (Mnt), obtained from Middle Anatolia, was purified according to the method used in a previous study (Özdemir *et al*., 2010). The organic impurities were removed using hydrogen peroxide, and the Mnt was dried at 95ºC and then pulverized to pass through a 595 μm sieve.

The purified Mnt was subjected to XRD analyses to check the crystal structure. The results of the powder XRD analysis revealed that the mineral was a Na-rich Mnt showing 001, 002, and 003 reflections. The CEC of the Na-Mnt was 0.68 meq/g Mnt (Özdemir *et al*., 2010).

The cetylpyridinium chloride monohydrate ($C_{21}H_{38}ClN{\cdot}H_2O$, MW = 358.01 g/mol) was purchased from Merck and the N-lauroyl sarcosinate sodium salt ($C_{15}H_{28}NNaO_3$, MW = 293.38 g/mol) from Sigma-Aldrich. They were of analytical grade and were used as received.

### *Methods*

The Mnt-CP-SR was prepared in two steps, with various amounts of CP/SR added in each step (Table 1). In the first step, $CP^+$ in amounts equivalent to 0.7 or 1.4 times the CEC of the Na-Mnt in a 1:50 aqueous suspension at 25ºC was shaken at 175 rpm in polypropylene tubes for 24 h. In the second step, the SR was added in different proportions to the CP-Mnt in an aqueous mixture and shaken for a further 24 h. Two samples (Mnt0.7CP0.7SR and Mnt0.7CP+0.35CP0.35SR, respectively) were prepared by the simultaneous addition of CP and SR on Mnt and on 0.7 CP-Mnt and were shaken for 48 h. All products were separated from the supernatants by filtering with Whatman™ filter papers. The solids obtained were rinsed using deionized water in a beaker and the free water was removed in an oven at 40ºC to allow the diffusion of SR into Mnt. After removal of the free water, the sample was dried at 60ºC. In previous studies monolayer adsorption was found to occur on the Mnt at

https://doi.org/10.1346/CCMN.2015.0630203 Published online by Cambridge University Press

Table 1. The amounts of CP + SR added in the preparation of SR-CP-Mnt samples.

| Sample | First step | Second step |
|---|---|---|
| Mnt0.7CP+0.7SR | 0.7 CEC CP | 0.7 CEC SR |
| Mnt0.7CP0.7SR | 0.7 CEC CP + 0.7 CEC SR | – |
| Mnt1.4CP+1.4SR | 1.4 CEC CP | 1.4 CEC SR |
| Mnt0.7CP+0.35CP0.35SR | 0.7 CEC CP | 0.35 CEC CP + 0.35 CEC SR |
| Mnt1.4CP+0.7SR | 1.4 CEC CP | 0.7 CEC SR |
| Mnt0.7CP+1.4SR | 0.7 CEC CP | 1.4 CEC SR |

0.7 CEC CP, and almost no CP remains in the solution. The adsorption of SR, however, is an equilibrium-driven process and 90−95% of the initial concentration adsorbs onto the CP-Mnt. The amounts of CP/SR added in the first and second steps are listed in Table 1. The samples were named in accordance with the amounts of CP + SR added. If the substrate was CP-Mnt it was separated by '+' from the component added. According to this definition, Mnt07CP+0.7SR means 0.7 CEC SR was added to 0.7 CP-Mnt. Mnt07CP0.7SR indicates that Mnt is added to the 0.7 CEC CP and 0.7 CEC SR solution.

The existence of liquid-crystal phases was detected using a polarized optical microscope (POM) (Olympus BX51/52-p, USA) equipped with a camera system. The thin films were prepared between microscope coverslips by dropping the solutions and waiting for 5 min for evaporation. The samples were placed between crossed polarizers in the POM. Areas with different contrast in the imaged texture correspond to domains where liquid crystals are oriented in different directions.

The TG experiments on Mnt-CP-SR samples, prepared in different proportions with CP and SR, were conducted using a TA Instruments model SDT Q600 (USA), with alumina as a reference. Samples weighing 15 mg were placed in Pt crucibles and heated from 30 to 800ºC at a scanning rate of 10ºC/min in an air atmosphere.

Electrokinetic potentials were determined using a Brookhaven 90Plus/Bi-MAS (Brookhaven Instruments Corp., New York, USA) with the electrophoretic mobility function. The electrophoretic mobility values obtained were calculated automatically to zeta-potential values using the Smoluchowski equation (Pecini and Avena, 2013). The zeta potential was measured using a 16 V/cm electric field, a 15 mA current, and 21 counts. For each determination, 40 mg of sample was dispersed in 40 mL of a $10^{-3}$ M KCl solution, used as inert electrolyte, and the slurry was then stirred. To generate zeta potential *vs.* pH curves, the suspension pH was adjusted using drops of $10^{-2}$ M HCl or KOH followed by magnetic stirring until equilibrium was attained (10 min).

The XRD patterns were recorded on randomly oriented powder samples, from 3 to 40º 2θ continuously at a scan rate of 2º/min, using a Rigaku Ultima-IV X-ray diffractometer (Rigaku Corp., Tokyo, Japan) operated at 35 kV and 30 mA with CuKα radiation.

## RESULTS AND DISCUSSION

The strong interaction between the anionic and cationic surfactant mixtures is pronounced and previous studies showed that oppositely-charged single-tailed surfactants could associate to form water-insoluble ion-pair amphiphiles known as coacervates (Kaler *et al.*, 1989; Herrington *et al.*, 1993; Zhu *et al.*, 2006). The solution and interfacial behavior of sodium dodecylsulfate and n-alkyltrimethylammonium bromide homologs were studied by Maiti *et al.* (2010) who reported the formation of needle-shaped crystals only for $C_{10}TA^{+}DS^{-}$ and $C_{12}TA^{+}DS^{-}$; for the larger carbon numbers in the hydrophobic chain, the occurrence of flower-like structures as well as needle-shaped crystals was reported. The shape and the size of the crystals depend on $C_{n,}$ and the size increased linearly with the alkyl chain lengths except for $C_{12}TA^{+}DS^{-}$.

The amounts of CP and SR used in the immobilization and also in the solutions were far greater than the critical micelle concentration (CMC) values of the surfactants (0.9 and 14.6 × $10^{-3}$ M, respectively; Srivastava and Ismail, 2014; Ghosh and Dey, 2011) and therefore the formation of aggregates in the solution was expected. A series of solutions containing pure SR at 0.95 M concentration which was ~ 65 times that of the CMC and CP-SR mixtures was prepared (Table 2), and images were acquired using POM (Figure 1).

Table 2. Properties of the solutions.

| SAMPLE | Solution property | Concentration |
|---|---|---|
| 1.4SR | Single component SR | 1.4 CEC SR |
| 0.35CP0.35SR | Mixture in equimolar amounts | 0.35 CEC CP+0.35 CEC SR |
| 0.7CP0.7SR | Mixture in equimolar amounts | 0.7 CEC CP+0.7 CEC SR |

https://doi.org/10.1346/CCMN.2015.0630203 Published online by Cambridge University Press

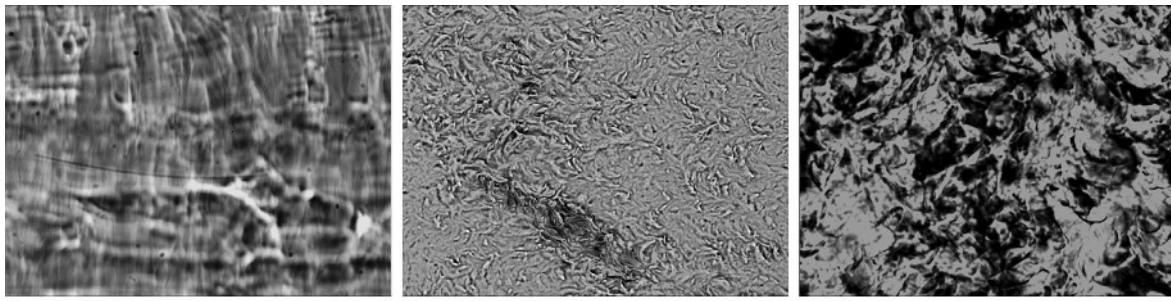


Figure 1. POM images of the CP-SR in the solution (samples 1.4SR, 0.35CP0.35SR, and 0.7CP0.7SR).

The aggregates formed in the SR solution (Figure 1) had a shape that was quite different from the spherical micellar geometry of the SR observed at its CMC (Ray *et al*., 2009). The POM images of the samples 0.35CP0.35SR and 0.7CP0.7SR revealed that the structures formed in each case were different from the structure formed in the pure SR solution. For sample 0.35CP0.35SR, needle-shaped crystals similar to those of $C_{12}TA^+DS^-$ were formed, although CP has a pyridine ring and a larger number of carbons ($n$ = 21). In the case of 0.7CP0.7SR, the structure became more complex and a leaf-like structure with curly margins was observed. The similarities observed indicated the formation of coacervate in the CP-SR mixtures in the solution phase.

The TG analyses (Table 3) indicated three mass-loss regions. The first, from 30 to 150ºC, was assigned to the dehydration of physically adsorbed water and water molecules around the metal cations on the exchangeable sites on the Mnt (Li and Ishida, 2003). The other two – 150–400ºC and 400–800ºC – were attributed, respectively, to the decomposition or de-surfactant temperature that is 353.4ºC when CP was Mnt-exchanged at 1.0 CEC, and to the thermal dehydroxylation of CP-Mnt and thermal decomposition of CP at 667ºC (Li *et al.*, 2006). The water content in the ternary systems studied (Mnt-CP-SR) was less than in Mnt (9.90%) which is in agreement with Hedley *et al.* (2007). The water content decreased to ~3% for samples with CP exchanged in amounts close to or greater than the CEC of the Mnt (Li *et al.*, 2006), whereas for samples with the CP exchanged less than the CEC, a 1% increase with respect to previous samples reflected the smaller amount of CP exchanged.

The de-surfactant temperature, obtained from the derivative-TG (DTG) curves, was 309ºC for samples with 0.7 CEC CP initially exchanged, and an intensity increase can be seen with the increase in the amount of SR. Naranjo *et al.* (2013) assigned the low-temperature mass-loss region (150–400ºC) for hexadecyltrimethylammonium (HDTMA)-surfactant adsorption on Mnt to a weak affinity produced at the external surface, in which the surfactant in the solution interacts, through the van der Waals forces, with the alkyl tails of previously adsorbed surfactant cations. In the Mnt-CP-SR samples with the CP initially exchanged at amounts greater than the CEC, two maxima, at 280 and 305ºC, were identified, an enlargement of the curves and a similar intensity increase with the amount of SR as for previous samples. These data are in agreement with those of Xi *et al.* (2007) and Vazquez *et al.* (2008) who indicated that the thermal stability of organoclays decreases with increased loading of surfactant. Two more maxima at 470 and 617ºC were found for the Mnt-CP-SR samples, which could be assigned to a high affinity between the solute and the adsorbent, related also to the high adsorption energy (Naranjo *et al.*, 2013).

Evaluation of the TG curves suggested the configuration and also the structure formed. The data for the second mass-loss region (Table 3) could also be used as a rough estimate of the amount of surfactant ($X$) which

Table 3. Thermal mass-loss of samples determined by TG at different temperature intervals.

| Sample | — Clay percentage of initial weight — | | |
|---|---|---|---|
| | 30–150ºC | 150–400ºC | 400–800ºC |
| Mnt | 9.90 | 0.92 | 4.51 |
| Mnt 0.7CP+0.7SR | 4.01 | 11.26 | 11.07 |
| Mnt 0.7CP 0.7SR | 4.08 | 12.47 | 10.94 |
| Mnt 1.4CP+1.4SR | 2.99 | 20.54 | 14.98 |
| Mnt 0.7CP+0.35CP 0.35SR | 2.33 | 13.87 | 13.63 |
| Mnt 1.4CP+0.7SR | 2.68 | 17.04 | 16.40 |
| Mnt 0.7CP+1.4SR | 3.89 | 13.84 | 10.75 |

https://doi.org/10.1346/CCMN.2015.0630203 Published online by Cambridge University Press

entered into the clay structure as suggested by Boeva *et al.* (2013). $X$ was found from Equation 1.

$$X = \frac{(mW)10^{-2}100}{((M-y)m(100-W)10^{-2}(84.22)10^{-3})} = \frac{(W10^{5})}{(84.22(M-y)(100-W))} \quad (1)$$

Where $m$ is the weight of the organoclay, $M$ is the molecular weight of the surfactant, and $W$ is the weight loss (%) of surfactant in organoclay. Using the Boeva *et al.* (2013) hypothesis to calculate a theoretical $X$ maximum and minimum produced by the presence of the surfactant counterion at 100 or 0%, the following values were found for CP loading when the SR remained at 100% (Table 4). At 0% SR, the values for CP loading obtained were greater than initially applied (from 5 to 10).

The different adsorption sites for swelling clays such as Mnt generate two different characteristic surfaces: inner (interlayer) and outer (external planar faces + edges) surfaces (Torres Sánchez *et al.*, 2011). Changes occurring on each of these surfaces could be assessed by zeta-potential measurements which show the electrostatic associations between the surfactants and the outer Mnt surface; and by measuring the $d_{001}$ values (XRD), changes in the interlayer space caused by the addition of surfactants can be inferred.

The zeta-potential measurements and suspension pH (Table 5) help to understand electrostatic association between both surfactants and the Mnt outer surface. The pH and zeta-potential value of Mnt obtained were in agreement with the data indicated for other raw montmorillonites (Thomas *et al.*, 1999; Maqueda *et al.*, 2013). The samples Mnt0.7CP+0.7SR and Mnt0.7CP+1.4SR had almost the same suspension pH and zeta-potential values, although the concentration of the SR solution was doubled for the preparation of the second sample in comparison with that used for the first (Table 5). The similar surface charge-behavior found for both samples could be assigned to limited association of SR up to 0.7 CEC on the complex CP-Mnt formed, while the contact of Mnt with a suspension of 0.7CP0.7SR, in sample Mnt0.7CP0.7SR, gave a suspension pH which was closer to that of Mnt (Table 5) but a zeta-potential value which was less negative.

Table 4. Estimated amount of CP loaded when SR remained 100%.

| Sample | pH |
|---|---|
| Mnt0.7CP+0.7SR | 0.61 |
| Mnt0.7CP 0.7SR | 0.69 |
| Mnt1.4CP+1.4SR | 1.25 |
| Mnt0.7CP+0.35CP 0.35SR | 0.78 |
| Mnt1.4CP+0.7SR | 0.99 |
| Mnt0.7CP+1.4SR | 0.77 |

Table 5. pH of the suspension with KCl $10^{-3}$M and zeta potential.

| Sample | pH | Zeta potential (mV) |
|---|---|---|
| Mnt | 7.35 | −32.3 |
| Mnt0.7CP+0.7SR | 6.41 | −37.2 |
| Mnt0.7CP 0.7SR | 6.75 | −23.2 |
| Mnt1.4CP+1.4SR | 6.21 | −27.4 |
| Mnt0.7CP+0.35CP 0.35SR | 6.33 | −24.7 |
| Mnt1.4CP+0.7SR | 6.45 | −23.2 |
| Mnt0.7CP+1.4SR | 6.44 | −32.3 |

The changes in zeta potentials with pH (Figure 2) revealed that the samples could be divided into two groups according to their response to the pH change. The zeta potential of raw Mnt was negative over the entire range of pH studied and ~25 mV (Thomas *et al.*, 1999). The electric charge developed from the outer surface of sample Mnt0.7CP+0.7SR was slightly more negative than that of Mnt. To explain this behavior, if only $CP^+$ interacted with the surface, the negative electric charges of the resulting product would decrease due to the formation of a surface-surfactant bilayer (Kung and Hayes, 1993) because they would produce cationic surfactants on the Mnt surface (Bianchi *et al.*, 2013), and a less negative surface charge than that of the Mnt would be determined. Further interaction of SR with the previous complex (0.7 CP-Mnt) to attain sample Mnt0.7CP+0.7SR at a pH of 6.41 (Table 5), however, indicated that the SR was negatively charged (anion) and could associate with the 0.7 CP-Mnt complex only by the positively charged surface groups. These surface groups are positive head groups of $CP^+$ (ammonium group) of the surfactant bilayer formed, and Al and Si of the Mnt edge (~3% of the total surface, $IEP_{pH}$ of edge = 7; Durán *et al.*, 2000).

Neutralization of the $CP^+$ surfactant bilayer by SR would shift the surface charge value of Mnt0.7CP+0.7SR sample closer to that of Mnt, while neutralization of the Mnt positive edge sites would increase the negative charge of the Mnt0.7CP+0.7SR relative to the Mnt sample, as shown in Figure 2. For SR in Mnt0.7CP+1.4SR compared to Mnt0.7CP+0.7SR, however, the TG analysis indicated a greater mass loss, and did not generate larger negative charge. The less negative zeta-potential value of the Mt0.7CP0.7SR relative to the Mnt sample was attributed to the micelles/coarcervates of CP-SR which produced a lesser neutralization of positive-edge charge of the Mnt.

The sample Mnt0.7CP0.7SR showed charge behavior similar to previous samples (Mnt0.7CP+0.7SR, Mnt0.7CP+1.4SR, and Mnt) while a suspension with a slightly higher pH value was found (Table 5). This pH behavior could be attributed to the formation of the CP-SR micelles/coacervates, leaving the suspension pH

https://doi.org/10.1346/CCMN.2015.0630203 Published online by Cambridge University Press

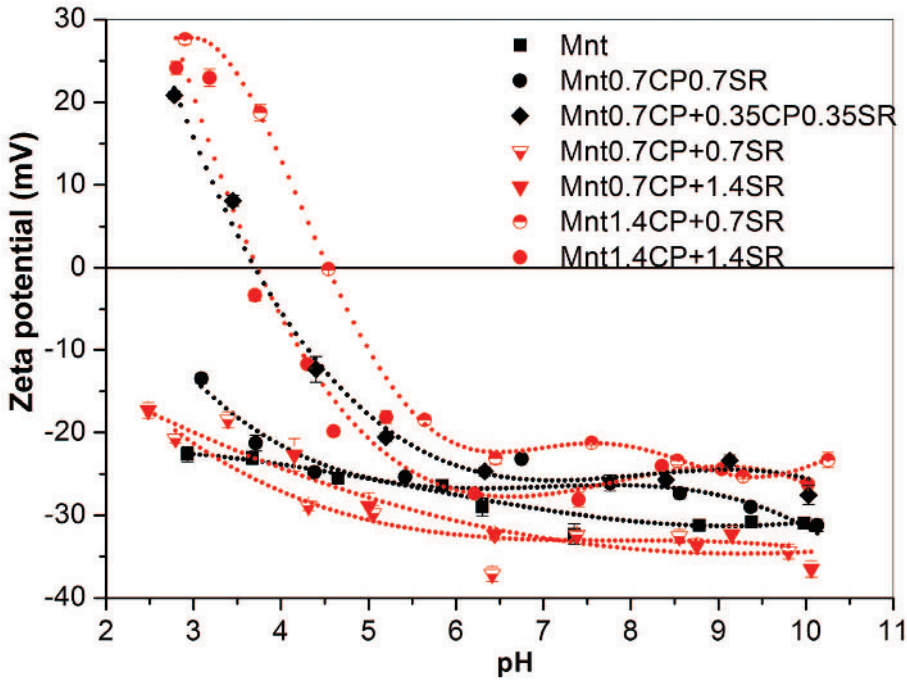


Figure 2. Zeta-potential curves of the samples.

close to that of the Mnt sample. At this pH, not as many positive edge sites were neutralized by the SR as in the sample Mnt0.7CP+0.7SR, and the zeta potential of the Mnt0.7CP0.7SR sample was less negative than the Mnt sample. The charge behavior of Mnt0.7CP0.7SR could be differentiated at values below and above pH 3.5 relative to the three previous samples. Taking into account that the carboxylate group of $SR^-$ has a $pK_a$ = 3.6 at a pH value of <3.6, it is neutral and the micelle structure with $CP^+$ is destabilized (Ghosh and Dey, 2011). Consequently the presence of free $CP^+$ neutralized the Mnt negative surface charge up to a pH 3.5 and above this pH a similar negative surface charge could be found for all these samples.

The samples Mnt1.4CP+1.4SR, Mnt0.7CP+0.35CP0.35SR, and Mnt1.4CP+0.7SR exhibited almost the same charge behavior in the pH range studied and also the isoelectric points could be inferred at a pH range from 4.0 to 5.0. The electric charge found for sample Mnt1.4CP+0.7SR was positive up to pH = 4.7 and less negative than Mnt above that pH value. Because the amount of $CP^+$ used in sample Mnt1.4CP+0.7SR was greater than the CEC of the Mnt, the negative charge of the Mnt was first neutralized as cationic surfactants covered the surface, and then a positive surface charge by tail-head type association of the surfactant formed (Naranjo *et al*., 2013). The suspension pH of sample Mnt0.7CP+0.35CP0.35SR was 6.33, very close to the values found for the samples Mnt0.7CP+0.7SR, Mnt1.4CP+0.7SR, and Mnt0.7CP+1.4SR (Table 5). In addition, this sample exhibited a similar charge behavior to that shown by samples Mnt1.4CP+1.4SR and Mnt1.4CP+0.7SR, indicating that the amount of $CP^+$ (0.7 CEC) leads to a very similar surface charge behavior regardless of the further addition of SR or mixtures of SR+CP.

The $d_{001}$ values of the samples (Figure 3) were compared to those of the samples prepared in a previous study (Özdemir *et al*., 2013) using only CP. The previously prepared samples were named as the host because they contain the same amount of CP as the new samples. No linear relationship among the host materials, amount of surfactants, and interlayer spacing were observed (Table 6). The triple interactions among the Mnt surface, CP, and SR were more complex than the double interactions between the Mnt and cationic surfactant.

Intercalation of cationic surfactants into the Mnt interlayers proceeds through ion exchange and the ionic polarity of the surfactants, an important factor in successful ion exchange (Mao *et al*., 2010). The interlayer spacing changed depending on the procedure followed during the preparation, when 0.7 CP-Mnt was used as a precursor (Table 6). Although the interlayer spacing increased from 1.29 nm to 1.54 nm for the sample Mnt0.7CP+0.7SR in comparison to the raw clay, this increase was less than that of the host (0.7 CP-Mnt) having a 1.79 nm interlayer spacing. The same behavior was also reported by Mao *et al*. (2010) during the preparation of mesoporous silica pillared clay using catanionic surfactant mixtures. They explained this behavior by the increase in the van der Waals forces

https://doi.org/10.1346/CCMN.2015.0630203 Published online by Cambridge University Press

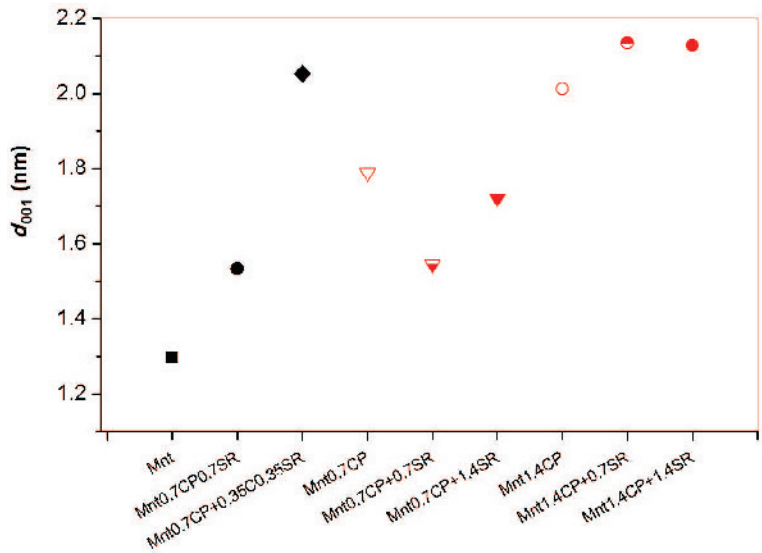


Figure 3. The $d_{001}$ values of the samples compared with the CP-Mnt.

between hydrocarbon chains and a decrease in the cationic electrostatic repulsion between the head groups of the cationic surfactant by the addition of an anionic surfactant (Mao *et al*., 2010). The XRD analyses of CP-Mnt showed that the pyridinium head groups were positioned and oriented randomly in the upper and lower margins of the surfactant monolayer (Özdemir *et al*., 2013). Thus, the randomly oriented head groups will interact easily with the negatively charged head group of SR to cause a decrease in the cationic repulsion between the head groups and formation of a more compact structure in the gallery region.

Although the orders for addition of the CP and SR were different in the Mnt0.7CP+0.7SR and Mnt0.7CP0.7SR samples, they have the same interlayer spacing. This indicates the dominant role of $CP^+$ in the formation of the surface structure, which was also confirmed by the zeta-potential measurements obtained for the external surface.

The interlayer spacing of sample Mnt0.7CP+ 0.35CP0.35SR, being greater than that of the host (0.7 CP-Mnt, $d_{001}$ = 1.79 nm), points to the formation of an arrangement changing between bi- and pseudo trimolecular layers (Lagaly *et al*., 2006). When the interlayer spaces of samples Mnt0.7CP+0.7SR and Mnt0.7CP+ 0.35CP0.35SR were considered, the greater interlayer spacing of the latter was attributed to the increase in the amount of CP. The interactions between previously adsorbed CP and the needle-like structure of CP-SR from the solution determine the orientation of ions and thus the interlayer spacing. The zeta-potential measurements and XRD analysis showed the distribution of $CP^+$ and $SR^-$ between external and interlayer surfaces, and further addition of the CP+SR mixture considerably affects both the structure of the interlayer and external surface charge.

The sample Mnt0.7CP+1.4SR has an interlayer spacing value between those of samples Mnt0.7CP+0.7SR

Table 6. Interlayer spacing of the samples indicated.

| Sample | Host Material | Materials and amounts added (equivalent CEC) | Interlayer spacing (nm) |
|---|---|---|---|
| **Host 1** | **Raw Clay** | – | **1.29** |
| Mnt0.7CP0.7SR | Raw clay | 0.7 CEC CP-0.7 CEC SR | 1.53 |
| **Host 2** | **0.7 CP-Mnt** | – | **1.79** |
| Mnt0.7CP+0.7SR | 0.7 CP-Mnt | 0.7 CEC SR | 1.54 |
| Mnt0.7CP+0.35CP0.35SR | 0.7 CP-Mnt | 0.35 CEC CP- 0.35 CEC SR | 2.05 |
| Mnt0.7CP+1.4SR | 0.7 CP-Mnt | 1.4 CEC SR | 1.72 |
| **Host 3** | **1.4 CP-Mnt** | – | **2.01** |
| Mnt1.4CP+1.4SR | 1.4 CP-Mnt | 1.4 CEC SR | 2.13 |
| Mnt1.4CP+0.7SR | 1.4 CP-Mnt | 0.7 CEC SR | 2.13 |

https://doi.org/10.1346/CCMN.2015.0630203 Published online by Cambridge University Press

and Mnt0.7CP+0.35CP0.35SR. The zeta-potential measurements indicated that sample Mnt0.7CP+1.4SR had an external surface structure similar to those of Mnt, Mnt0.7CP+0.7SR and Mnt0.7CP0.7SR. Consequently, the addition of more SR did not affect the CP-SR complex formed at the external surface but did affect the internal surface.

When 1.4 CP-Mnt was used as the host, the interlayer spaces of the samples Mnt1.4CP+1.4SR and Mnt1.4CP+0.7SR were almost the same, and a slight increase was observed in comparison to the host. This implied that the main contribution to the increase in interlayer spacing in the resulting organoclay was from the cationic surfactant (Chen *et al*., 2008).

## CONCLUSIONS

The strong interaction between the CP and SR in the aqueous medium, and the coacervate formation due to this interaction, are known. The addition of Mnt to the CP and SR in aqueous media changed their interaction. The Mnt surface charge dominated the interaction with $CP^+$, and the addition of SR affected the interlayer and surface properties of Mnt differently. The SR added to the CP-Mnt reduced the $d_{001}$ interlayer spacing, compared to that of CP-Mnt, whereas the same addition caused an insignificant change in the zeta potential of the Mnt-CP-SR. The amount of CP added played a major role in the change of the $d_{001}$ interlayer spacing as well as the zeta potential of the samples. These results indicate that the interaction of SR with CP was relatively weak on the external surface, whereas these interactions were strong enough in the interlayer to cause a considerable change in the interlayer structure compared to the CP-Mnt. The external and interlayer surface properties of the new material formed are rather different from those of the organoclays prepared with a single cationic surfactant. The variation of the external surface charge from negative to positive with the change in pH allows a wide range of applicability. For instance, samples 0.7CP+0.35CP0.35SR, 1.4CP+0.7 SR, and 1.4 CP+1.4 SR could be used in the adsorption of both anionic and cationic species, depending on the pH. The strong interaction between the cationic and anionic surfactants and Mnt in the interlayer surface allows the possibility of the complex to capture and retain various organic materials.

## ACKNOWLEDGMENTS

The authors acknowledge gratefully the support of the Reseach Project Fund of Ege University through project number 13-MUH-035.

## REFERENCES

Bianchi, A.E., Fernández, M., Pantanetti, M., Viña, R., Torriani, I., Torres Sánchez, R.M., and Punte, G. (2013) $ODTMA^+$ and $HDTMA^+$ organo-montmorillonites characterization: New insight by WAXS, SAXS and surface charge. *Applied Clay Science*, **83-84**, 280–285.

Boeva, N.M., Bocharnikova, Y.I., Nasedkin, V.V., Belousov, P. E., and Demidenok, K.V. (2013) Thermal analysis as an express method for assessing the quality and quantity of natural and synthesized organoclays. *Nanotechnologies in Russia*, **8**, 205–208.

Bramer, T., Dew, N., and Edsman, K. (2007) Pharmaceutical applications for catanionic mixtures. *Journal of Pharmacy and Pharmacology*, **59**, 1319–1334.

Caillet, C., Hebrant, M., and Tondre, C. (2000) Sodium octyl sulfate/cetyltrimethyl-ammonium bromide catanionic vesicles: aggregate composition and probe encapsulation. *Langmuir*, **16**, 9099– 9102.

Caruso, F. (2000) Hollow capsule processing through colloidal templating and self-assembly. *Chemistry – a European Journal*, **6**, 413–419.

Chen, D., Zhu, J.X., Yuan, S.J., Chen, T.-H., and He, H.P. (2008) Preparation and characterization of anion-cation surfactants-modified montmorillonite. *Journal of Thermal Analysis and Calorimetry*, **94**, 841–848.

Durán, J.D.G., Ramos-Tejeda, M.M., Arroyo, F.J., and González-Caballero, F. (2000) Rheological and electrokinetic properties of sodium montmorillonite suspensions: I. Rheological properties and interparticle energy of interaction. *Journal of Colloid and Interface Science*, **229**, 107–117.

Erkan, I., Alp, I., and Çelik, M.S. (2010) Characterization of organo-bentonites obtained from different linear-chain quaternary alkylammonium salts. *Clays and Clay Minerals*, **58**, 792–802.

Fischer, A., Hebrant, M., and Tondre, C. (2002) Glucose encapsulation in catanionic vesicles and kinetic study of the entrapment/release processes in the sodium dodecyl benzene sulfonate/cetyltrimethylammonium tosylate/water system. *Journal of Colloid and Interface Science*, **248**, 163–168.

Ghosh, S. and Dey, J. (2011) Interaction of sodium N-lauroylsarcosinate with N-alkylpyridinium chloride surfactants: Spontaneous formation of pH responsive, stable vesicles in aqueous mixtures. *Journal of Colloid and Interface Science*, **358**, 208–216.

Hedley, C.B., Yuan, G. and Theng, B.K.G. (2007) Thermal analysis of montmorillonites modified with quaternary phosphonium and ammonium surfactants. *Applied Clay Science*, **35**, 180–188.

Hentze, H.P., Raghavan, S.R., McKelvey, C.A., and Kaler, E.W. (2003) Silica hollow spheres by templating of catanionic vesicles. *Langmuir*, **19**, 1069–1074.

Herrington, K.L., Kaler, E.W., Miller, D.D., Zasadzinski, J.A., and Chiruvolu, S. (1993) Phase behavior of aqueous mixtures of dodecyltrimethylammonium bromide (DTAB) and sodium dodecyl sulfate (SDS). *Journal of Physical Chemistry*, **97**, 13792–13802.

Kaler, E.W., Murthy, A.K., Rodriguez, B.E., and Zasadzinski, J.A.N. (1989) Spontaneous vesicle formation in aqueous mixtures of single-tailed surfactants. *Science*, **245**, 1371–1374.

Karande, P., Jain, A., Arora, A., Ho, M.J., and Mitragotri, S. (2007) Synergistic effects of chemical enhancers on skin permeability: A case study of sodium lauroylsarcosinate and sorbitan monolaurate. *European Journal of Pharmaceutical Sciences*, **31**, 1–7.

Kung, K.-H.S. and Hayes, K.F. (1993) Fourier transform infrared spectroscopic study of the adsorption of cetyltrimethylammonium bromide and cetylpyridinium chloride on silica. *Langmuir*, **9**, 263–267.

Lagaly, G., Ogawa, M., and Dekany, I. (2006) Clay mineral organic interactions. P. 328 in: *Handbook of Clay Science* (F. Bergaya, B.K.G. Theng, and G. Lagaly, editors),

Elsevier, Amsterdam.
Lasic, D.D. (1998) Novel applications of liposomes. *Trends in Biotechnology*, **16**, 307–321.
Li, Y. and Ishida, H. (2003) Concentration-dependent conformation of alkyl tail in the nanoconfined space: Hexadecylamine in the silicate galleries. *Langmuir*, **19**, 2479–2484.
Li, J., Zhu, L., and Cai, W. (2006) Characteristics of organobentonite prepared by microwave as a sorbent to organic contaminants in water. *Colloids and Surfaces A: Physicochemical Engineering Aspects*, **281**, 177–183.
Maiti, K., Bhattacharya, S.C., Moulik, S.P., and Panda, A.K. (2010) Physicochemical studies on ion-pair amphiphiles: Solution and interfacial behavior of systems derived from sodium dodecyl sulfate and n-alkyltrimethylammonium bromide homologues. *Journal of Chemical Science*, **122**, 867–879.
Mao, H., Li, B., Li, X., Yue, L., Liu, Z., and Ma, W. (2010) Novel one-step synthesis route to ordered mesoporous silica-pillared clay using cationic-anionic mixed-gallery templates. *Industrial and Engineering Chemistry Research*, **49**, 583–591.
Maqueda, C., dos Santos Afonso, M., Morillo, E., Torres Sánchez, R.M., Perez-Sayago, M., and Undabeytia, T. (2013) Adsorption of diuron on mechanically and thermally treated montmorillonite and sepiolite. *Applied Clay Science*, **72**, 175–183.
McKelvey, C.A., Kaler, E.W., Zasadzinski, J.A.N., Coldren, B., and Jung, H.T. (2000) Templating hollow polymeric spheres from catanionic equilibrium vesicles: synthesis and characterization. *Langmuir*, **16**, 8285–8290.
Naranjo, P., Sham, E.L., Rodríguez Castellón, E., Torres Sánchez, R.M., and Farfán Torres, E.M. (2013) Identification and quantification of the interaction mechanisms between the cationic surfactant HDTMA-Br and montmorillonite. *Clays and Clay Minerals*, **61**, 98–106.
Özdemir, G., Hoşgör Limoncu, M., and Yapar, S. (2010) Antibacterial effect of heavy metal and cetylpyridinium exchanged montmorillonites. *Applied Clay Science*, **48**, 319–323.
Özdemir, G., Yapar, S., and Hoşgör Limoncu, M. (2013) Preparation of cetylpyridinium montmorillonite for antibacterial applications. *Applied Clay Science*, **72**, 201–205.
Parolo, M.E., Avena, M.J., Pettinari, G., Zajonkovsky, I., Valles, J.M., and Baschini, M.T. (2010) Antimicrobial properties of tetracycline and minocycline-montmorillonites. *Applied Clay Science*, **49**, 194–199.
Pecini E.M. and Avena M.J. (2013) Measuring the isoelectric point of the edges of clay mineral particles: The case of montmorillonite. *Langmuir*, **29**, 14926–14934.
Rädler, J.O., Koltover, I., Salditt, T., and Safinya, C.R. (1997) Structure of DNA-cationic liposome complexes: DNA intercalation in multilamellar membranes in distinct interhelical packing regimes. *Science*, **275**, 810–814.
Ray, G.B., Ghosh, S., and Moulik, S.P. (2009) Physicochemical studies on the interfacial and bulk behaviors of sodium *N*-dodecanoyl sarcosinate (SDDS). *Journal of Surfactants and Detergents*, **12**, 131–143.
Ruiz-Hitzky, E., Aranda, P., Darder, M., and Rytwo, G. (2010) Hybrid materials based on clays for environmental and biomedical applications. *Journal of Materials Chemistry*, **20**, 9306–9321.
Schumann, D., Hesse, R., Sears, S.K., and Vali, H. (2014) Expansion behavior of octadecylammonium-exchanged low to high-charge reference smectite-group minerals as revealed by high-resolution transmission electron microscopy on ultrathin sections. *Clays and Clay Minerals*, **62**, 336–353.
Srivastava, A. and Ismail, K. (2014) Characteristics of mixed systems of phenol red and cetylpyridinium chloride. *Journal of Molecular Liquids*, **200**, 176–182.
Svenson, S. (2004) Controlling surfactant self assembly. *Current Opinion in Colloid and Interface Science*, **9**, 201–202.
Thomas, F., Michot, L.J., Vantelon, D., Montarges, E., Prelot, B., Cruchaudet, M.J., and Delon, F. (1999) Layer charge and electrophoretic mobility of smectites. *Colloids and Surfaces A: Physicochemical and Engineering Aspects*, **59**, 351–358.
Tondre, C. and Caillet, C. (2001) Properties of the amphiphilic films in mixed cationic/anionic vesicles: a comprehensive view from a literature analysis. *Advances in Colloid and Interface Science*, **93**, 115–134.
Torres Sánchez, R.M., Genet, M.J., Gaigneaux, E.M., dos Santos Afonso, M., and Yunes, S. (2011) Benzimidazole adsorption on the external and interlayer surfaces of raw and treated montmorillonite. *Applied Clay Science*, **53**, 366–373.
Vazquez, A., López, M., Kortaberria, G., Martínand, L., and Mondragon, I. (2008) Modification of montmorillonite with cationic surfactants. Thermal and chemical analysis including CEC determination. *Applied Clay Science*, **41**, 24–36.
Xi, Y., Frost, R.L., and He, H. (2007) Modification of the surfaces of Wyoming montmorillonite by the cationic surfactants alkyl trimethyl, dialkyl dimethyl, and trialkyl methyl ammonium bromides. *Journal of Colloid and Interface Science*, **305**, 150–158.
Zhu, Z., Xu, H., Liu, H., Gonzalez, Y.I., Kaler, E.W., and Liu, S. (2006) Stabilization of catanionic vesicles via polymerization. *Journal of Physical Chemistry B*, **110**, 16309–16317.

(*Received 16 September 2014; revised 18 March 2015; Ms. 914; AE: H. He*)